



# 1 Increased accuracy and precision in igneous and detrital zircon 2 geochronology using CA-LA-ICPMS

3

4 Erin E. Donaghy<sup>1</sup>, Michael P. Eddy<sup>1</sup>, Federico Moreno<sup>2</sup>, Mauricio Ibañez-Mejía<sup>2</sup>

5 <sup>1</sup>Department of Earth, Atmospheric, and Planetary Sciences, Purdue University, West Lafayette, 47907, United  
6 States of America

7 <sup>2</sup>Department of Geosciences, University of Arizona, Tucson, 85721, United States of America

8

9 *Correspondence to:* Erin E. Donaghy (edonaghy@purdue.edu)

10

11 **Abstract.** Detrital zircon geochronology by laser ablation-inductively coupled plasma-mass spectrometry (LA-ICP-  
12 MS) is a widely-used tool for determining maximum depositional ages, sediment provenance, and reconstructing  
13 sediment routing pathways. Although the accuracy and precision of U-Pb geochronology measurements has  
14 improved over the past two decades, Pb-loss continues to impact the ability to resolve zircon age populations by  
15 biasing affected zircon toward younger apparent ages. Chemical abrasion (CA) has been shown to reduce or  
16 eliminate the effects of Pb-loss in zircon U-Pb geochronology, but has yet to be widely applied to large-n detrital  
17 zircon analyses. Here, we assess the efficacy of the chemical abrasion treatment on zircon prior to analysis by LA-  
18 ICP-MS and discuss the advantages and limitations of this technique in relation to detrital zircon geochronology. We  
19 show that i) CA does not systematically bias LA-ICP-MS U-Pb dates for thirteen reference materials that span a  
20 wide variety of crystallization dates and U concentrations; ii) CA-LA-ICP-MS U-Pb zircon geochronology can  
21 reduce, or eliminate, Pb-loss in samples that have experienced significant radiation damage; and iii) bulk CA prior to  
22 detrital zircon U-Pb geochronology by LA-ICP-MS improves the resolution of Neoproterozoic to present zircon age  
23 populations and the percentage of concordant analyses in Mesoproterozoic and older age populations. The selective  
24 dissolution of zircon that has experienced high degrees of radiation damage suggests that some detrital zircon age  
25 populations could be destroyed or have their abundance significantly modified during this process. However, we did  
26 not identify this potential effect in either of the detrital zircon samples that were analyzed as part of this study. We  
27 conclude that pre-treatment of detrital zircon by bulk CA may be useful for applications that require increased  
28 resolution of detrital zircon populations.

29

## 30 1. Introduction

31 Detrital zircon U-Pb geochronology is a common and widely-used tool with a broad range of applications  
32 across multiple subdisciplines of geology. As the efficiency, accuracy, and precision of U-Pb geochronology  
33 measurements continue to improve (e.g., Carrapa, 2010; Gehrels, 2012; Gehrels, 2014; Pullen et al., 2014; Sundell et  
34 al., 2021), the production of large detrital zircon datasets by laser ablation-inductively coupled plasma-mass  
35 spectrometry (LA-ICP-MS) has become more common. In basin analysis and tectonics, these datasets are often used  
36 to determine sediment provenance, characterize source terranes, and reconstruct ancient sediment routing pathways  
37 (Fedo et al., 2003; Anderson 2005; Smith et al., 2023). The resulting data is typically interpreted using kernel density  
38 estimates (KDEs) or probability density plots (PDPs) and assessed by comparing the means, heights, widths, and  
39 modes of peaks in detrital zircon age spectra using similarity/dissimilarity metrics. One factor that may limit the



40 resolution of these peaks is Pb-loss which can smear zircon age populations toward younger apparent U-Pb dates. This  
41 issue may not bias data in which Pb-loss is a recent phenomenon provided that the  $^{207}\text{Pb}/^{206}\text{Pb}$  date is used for zircon  
42 crystallization. However, protracted or complicated histories of Pb-loss can make it difficult to interpret  $^{207}\text{Pb}/^{206}\text{Pb}$   
43 dates (Nemchin and Cawood, 2005) and many labs only use this system to constrain a zircon crystallization date if it  
44 is concordant. The precision of the  $^{207}\text{Pb}/^{206}\text{Pb}$  chronometer also typically limits its use to Mesoproterozoic and older  
45 zircon. The most precise date for Neoproterozoic or younger zircon is generally obtained with the  $^{206}\text{Pb}/^{238}\text{U}$   
46 chronometer, but these dates are more susceptible to open-system behavior. Zircon age populations that are affected  
47 by Pb-loss in this age range can be difficult to identify since Pb-loss trajectories closely follow Concordia and may  
48 result in analyses that are concordant within analytical uncertainty but have spuriously young  $^{206}\text{Pb}/^{238}\text{U}$  dates. The  
49 effect of Pb-loss on detrital zircon analyses is consequently two-fold. It reduces the number of concordant  
50 Mesoproterozoic and older zircons, making populations in this age range more difficult to identify, and it will  
51 cryptically smear Neoproterozoic and Phanerozoic zircon age populations along concordia toward spuriously young  
52 dates, making it difficult to resolve differences between distinct but similarly aged populations.

53 The chemical abrasion method, in which thermally annealed zircon is partially dissolved in hydrofluoric acid  
54 (HF) prior to analysis has been shown to successfully mitigate Pb-loss (e.g., Mundil et al., 2004; Mattinson, 2005;  
55 Widmann et al., 2019; Sharman and Malkowski, 2023) and is widely used in isotope dilution-thermal ionization-mass  
56 spectrometry (ID-TIMS) U-Pb zircon geochronology (*see reviews in* Schoene, 2014; Schaltegger et al., 2015). The  
57 technique likely benefits analyses in two ways. First, it selectively dissolves zones of the zircon crystal that have  
58 experienced extensive radiation damage and possible Pb-loss (Widmann et al., 2019). Second, the partial dissolution  
59 process dissolves inclusions that may harbor non-radiogenic Pb, leading to a higher proportion of zircon-hosted  
60 radiogenic Pb ( $\text{Pb}^*$ ) in the measured analysis. Over the last decade, several groups have analyzed chemically abraded  
61 zircon by LA-ICP-MS and shown that this approach can successfully mitigate Pb-loss, resulting in the increased  
62 concordance, precision, and, presumably, accuracy of U-Pb dates (Crowley et al., 2014; Von Quadt et al., 2014). These  
63 results suggest that chemical abrasion prior to large-n detrital zircon analyses may also be useful when the resolution  
64 of closely spaced Neoproterozoic and Phanerozoic peak age populations is desired or when high degrees of  
65 discordance obscure the interpretation of Mesoproterozoic and older age populations. Here, we assess the benefits and  
66 drawbacks of this pre-treatment with a particular focus on whether the resolution of younger zircon age populations  
67 is increased, whether it improves concordance for Precambrian detrital zircon populations, and/or whether the  
68 selective removal of metamict zircon will bias age populations.

69

## 70 2. U-Pb Zircon Geochronology Approach and Methods

71 We have divided our study into three distinct parts. First, we compare chemically abraded and untreated  
72 zircon from 13 zircon reference materials (Table 1) to test whether chemical abrasion systematically biases U-Pb dates  
73 analyzed by LA-ICP-MS. Crowley et al. (2014) demonstrated that chemically abraded zircon ablate more slowly and  
74 experience greater down-hole fractionation than untreated zircon. These differences are likely related to differences  
75 in the ability of the laser to couple with zircon that has been etched by the chemical abrasion process. While no  
76 negative effects of chemical abrasion were seen in Crowley et al. (2014) or von Quadt et al. (2014), provided that  
77 chemically abraded reference materials were used as primary standards, we have expanded the age range of reference



78 zircon analyzed to encompass 28.5 – 3467 Ma. This increased age range of the tested reference materials provides a  
 79 more complete understanding of LA-ICP-MS U-Pb systematics on chemically abraded zircon and whether a single  
 80 primary standard can be used for a wide range of zircon dates and U content. Second, we assess the ability of chemical  
 81 abrasion to mitigate Pb-loss in an igneous sample that has experienced substantial radiation damage by comparing  
 82 chemically abraded and non-chemically abraded  $^{206}\text{Pb}/^{238}\text{U}$  LA-ICP-MS zircon analyses to a newly produced CA-ID-  
 83 TIMS reference date for the same sample. Finally, we assess how CA affects detrital zircon (DZ) age spectra by  
 84 comparing chemically abraded and untreated aliquots of two detrital samples. One sample is Cenozoic in age and  
 85 contains both Phanerozoic (100-300 Ma) and Precambrian (1000-1200 Ma) zircon age populations, whereas the  
 86 second sample is Proterozoic and contains zircon age populations between 2000-3500 Ma.  
 87

**Table 1.** Zircon reference materials for U-Pb isotopic analyses

Name	ID-TIMS age (Ma)	2S	References	Host lithology	Quantity
Fish Canyon tuff	28.476	0.029	Schmitz and Bowring (2001) <sup>a</sup>	Dacite	Unlimited
GHR1	48.106	0.023	Eddy et al. (2019) <sup>b</sup>	Rapakivi Granite	Unlimited
49127	136.6		Gehrels et al. (2008) <sup>b</sup>		Uncertain
Plesovice	337.13	0.37	Slama et al. (2008) <sup>a</sup>	Potassic Granulite	Unlimited
Temora 2	418.37	0.14	Mattinson (2010) <sup>a</sup>	Gabbro	Unlimited
R33	420.53	0.16	Mattinson (2010) <sup>a</sup>	Monzodiorite	Unlimited
SLM	563.5	3.2	Gehrels et al. (2008) <sup>b</sup>	Single Crystal	Limited
SLF	555.86	0.68	Wang et al. (2022) <sup>b</sup>	Single Crystal	Limited
91500	1065.4	0.3	Wiedenbeck et al. (2008) <sup>b</sup>	Single Crystal	Limited
FC1	1098.47	0.16	Mattinson (2010) <sup>a</sup>	Gabbro	Unlimited
Oracle	1434	8	Gehrels et al. (2008) <sup>b</sup>	Granite	Uncertain
QGNG	1851.6	0.6	Black et al. (2004) <sup>b</sup>	Quartz gabbro gneiss	Uncertain
OG1	3467.05	0.63	Stern et al. (2009) <sup>a</sup>	Diorite	Unlimited

<sup>a</sup> Chemical abrasion CA-ID-TIMS

<sup>b</sup> Traditional ID-TIMS

88

89

90

## 91 2.1 Methods for Thermal Annealing and Chemical Abrasion

92

93

94

95

96

97

98

99

All chemically abraded zircon aliquots were treated at Purdue University following methods modified from Mattinson (2005) and similar to those described in Eddy et al. (2019). Zircon separates were first thermally annealed in quartz crucibles for 60 hours at 900°C in a muffle furnace and then loaded in 3 mL savillex hex beakers with ~1 mL of 28M HF and 0.1 mL of 8M HNO<sub>3</sub> for bulk chemical abrasion. Four hex beakers were then stacked in the PTFE liner for a 125 mL Parr acid dissolution vessel. To ensure vapor exchange during partial dissolution a small hole was drilled through each beaker cap. The fully assembled Parr acid dissolution vessel was then held at 210°C for 12 hours. Once the chemical abrasion process was completed, the leachate was removed from each beaker using a pipette and the zircons were rinsed three times with H<sub>2</sub>O. Chemically abraded aliquots were then sent to the University of Arizona



100 LaserChron Center (ALC) for mounting and LA-ICP-MS analyses. Methods for chemical abrasion of zircon prior to  
101 the ID-TIMS analyses reported in this paper are similar to those described above, except individual zircon were  
102 chemically abraded in 200  $\mu\text{L}$  Ludwig style microcapsules and repeatedly rinsed in distilled 7M HCl and ultrapure  
103  $\text{H}_2\text{O}$  prior to spiking and complete dissolution.

104

### 105 **2.2 LA-ICP-MS Zircon U-Pb Geochronology**

106 Zircon aliquots were mounted in 2.5-cm-diameter epoxy plugs, polished, and imaged by  
107 cathodoluminescence using a Hitachi 3400N SEM and a Gatan Chroma CL system prior to analysis by LA-ICP-MS.  
108 Chemically abraded zircon were only mounted with chemically abraded zircon reference materials, while untreated  
109 zircon aliquots were mounted with untreated reference materials. U-Pb isotopic analyses were obtained via LA-ICP-  
110 MS using a Thermo Element2 single-collector ICP-MS coupled with a Teledyne Photon Machines Analyte G2  
111 excimer laser at the ALC. The diameter of the laser spot was set to 30 microns. Elemental- and mass-dependent  
112 instrumental fractionation were corrected by bracketing unknown analyses with analyses of primary reference material  
113 FC1 following the methods described in Pullen et al. (2018). Only chemically abraded primary standards were used  
114 for calibration of chemically abraded samples and only untreated primary standards were used for untreated samples  
115 following the recommendations of Crowley et al. (2014). Bracketing occurred every 10-11 analyses for the round-  
116 robin comparison of zircon reference materials, every 2-3 analyses for igneous zircon analyses, and every 5 analyses  
117 for detrital zircon samples. Data reduction was completed using an in-house Matlab script, AgeCalcML v.1.42  
118 (Sundell et al., 2021). This program allows the user to filter data by maximum  $^{206}\text{Pb}/^{238}\text{U}$  and/or  $^{207}\text{Pb}/^{206}\text{Pb}$  uncertainty  
119 (typically set to 10%), reverse discordance (typically 5%), and normal discordance (typically 20%). For the purposes  
120 of this study, we de-activated all uncertainty and discordance filters in AgeCalcML and all isotopic data measured via  
121 LA-ICP-MS that is from clearly ablated zircon are reported in Tables S1-S13. However, age interpretations of igneous  
122 and detrital zircon data use filtered data (Tables S14-S19).

123

### 124 **2.3 CA-ID-TIMS Zircon U-Pb Geochronology**

125 Sample MIGU-02, a granitoid from the Guyana Shield, was analyzed by ID-TIMS at Purdue University to  
126 provide a reference date to compare the chemically abraded and untreated LA-ICP-MS analyses. Following the  
127 chemical abrasion methods described above, individual zircons were spiked with the EARTHTIME  $^{205}\text{Pb}$ ,  $^{233}\text{U}$ ,  $^{235}\text{U}$   
128 isotopic tracer (Condon et al., 2015; McLean et al., 2015) and loaded into a Parr acid digestion vessel with 28M HF.  
129 The vessel was then held at 210°C for 60 hours for zircon dissolution. After dissolution, the samples were dried down  
130 and then converted to chloride form, by adding 75  $\mu\text{L}$  7M HCl, reassembling the Parr acid digestion vessel, and holding  
131 it at 180°C for 12 hours. After conversion to chloride form, the solution was converted to 3M HCl in preparation for  
132 anion exchange chromatography. Pb and U were purified from these solutions using AG-1x8 anion exchange resin  
133 following procedures modified from Krogh (1973). The resulting aliquots were dried down to a chloride salt before  
134 being dissolved in silica gel, dried onto rhenium filaments, and loaded into an IsotopX Phoenix TIMS for analysis. Pb  
135 isotopic measurements were made by peak hopping on a Daly detector and corrected for mass dependent isotopic  
136 fractionation using an  $\alpha = 0.147 \pm 0.028$  (%amu) and deadtime = 29.9 ns, derived from repeat measurements of the



137 NBS981 Pb reference material. We assume that all  $^{204}\text{Pb}$  is from laboratory contamination and correct for it using a  
138 laboratory Pb isotopic composition of  $^{206}\text{Pb}/^{204}\text{Pb} = 18.82 \pm 0.74$  ( $2\sigma$ ),  $^{207}\text{Pb}/^{204}\text{Pb} = 15.52 \pm 0.63$  ( $2\sigma$ ),  $^{208}\text{Pb}/^{204}\text{Pb} =$   
139  $37.93 \pm 1.60$  ( $2\sigma$ ) derived from repeat total procedural blank measurements run during 2022. Uranium was run as an  
140 oxide ( $\text{UO}_2$ ) and isotopic measurements were made statically using Faraday detectors and corrected for fractionation  
141 using the known ratio of  $^{233}\text{U}/^{235}\text{U}$  in the EARTHTIME  $^{205}\text{Pb}$ - $^{233}\text{U}$ - $^{235}\text{U}$  isotopic tracer (Condon et al., 2015; McLean  
142 et al., 2015) and assuming a zircon  $^{238}\text{U}/^{235}\text{U}$  value of  $137.818 \pm 0.045$  (Hiess et al., 2012). Data reduction was done  
143 using the ET\_Redux software package (Bowring et al., 2011) and the decay constants of Jaffey et al. (1971). All  
144 isotopic data measured via CA-ID-TIMS are presented in Table S15.

145

146

### 147 3. Results

148

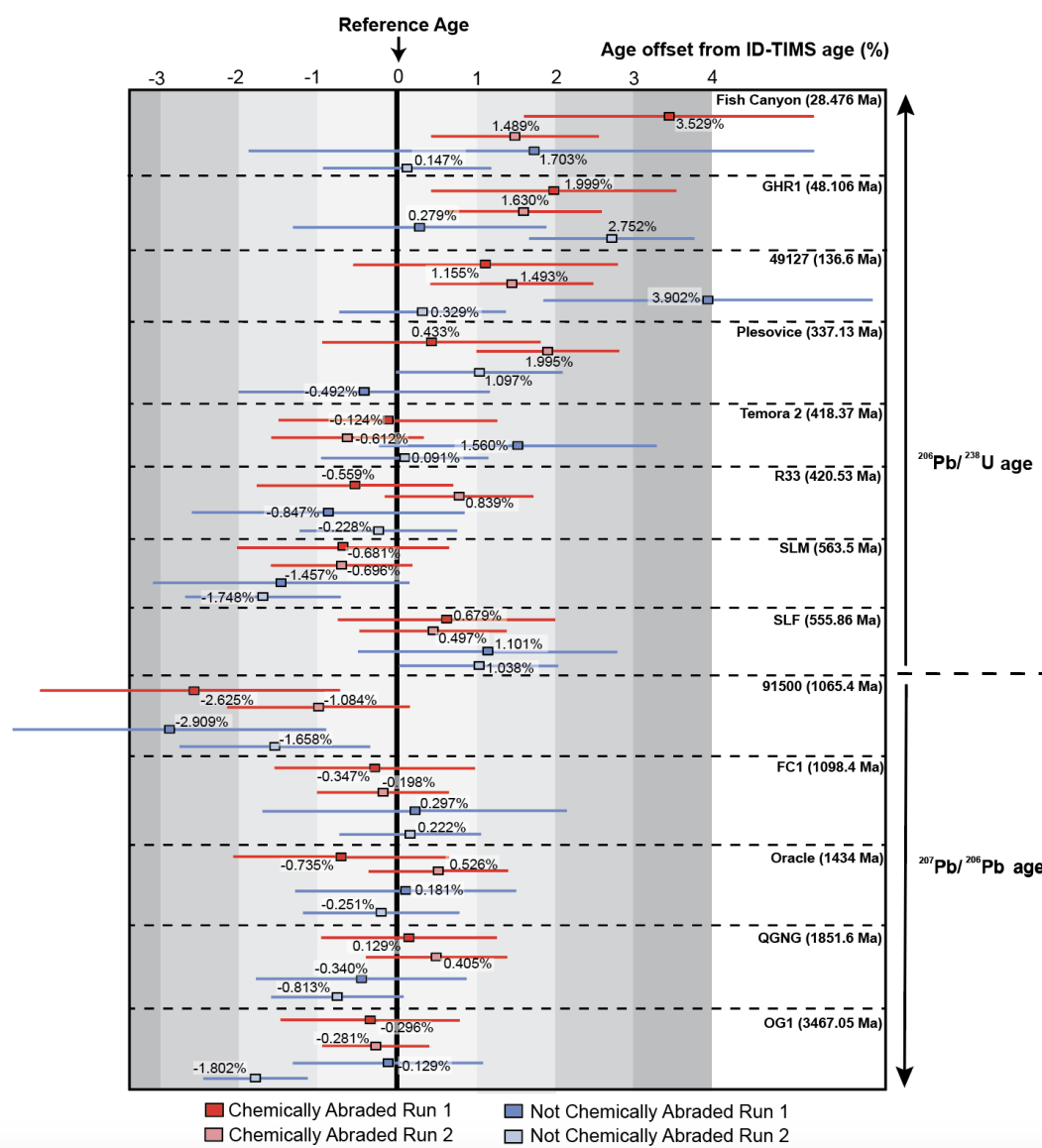
#### 149 3.1 CA-LA-ICP-MS U-Pb Geochronology of Zircon Reference Materials

150 Treated and untreated aliquots of thirteen different zircon U-Pb reference materials (Table 1) were analyzed in this  
151 study to further assess whether chemical abrasion systematically biases U-Pb dates. The reference materials were  
152 analyzed during two round-robin runs. The first run targeted 15 zircon grains from treated and untreated aliquot of  
153 reference materials. During the second run, 30 zircon grains were targeted. Because FC-1 was used as a primary  
154 reference material for calibration of the LA-ICP-MS, approximately 30 FC-1 zircons were analyzed during run 1 and  
155 87 were analyzed during run 2 per treated and untreated aliquots. The total number of zircons analyzed was 657 in  
156 each of the chemically abraded and untreated aliquots of reference materials. Of the 657 grains in the chemically  
157 abraded aliquot, 635 analyses (96.6%) were retained following filtering for discordance, whereas 608 analyses  
158 (92.5%) were retained in the untreated aliquot. These results further confirm that CA helps mitigate Pb-loss and  
159 improve precision in LA-ICP-MS analyses (e.g., Crowley et al., 2014; von Quadt et al., 2014). The most extreme  
160 change in concordance and data retention occurred between treated and untreated FC-1 zircon (1098.4 Ma). Of the  
161 117 grains analyzed per treated and untreated aliquot, 97.4% of analyses were retained in the chemically abraded  
162 aliquot versus 82.1% in the untreated aliquot. Discordance criteria used for filtering the above data were reverse  
163 discordance larger than 5% and/or  $^{206}\text{Pb}/^{238}\text{U}$  errors larger than 10%.

164 The dates of CA and non-CA reference materials are all within 0.1 – 4% of the reference ages determined  
165 by ID-TIMS (Fig. 1). Therefore, despite an increased concordance of treated grains relative to untreated grains,  
166 weighted means of acceptable analyses are indistinguishable and indicate that it is unlikely that chemical abrasion  
167 biases U-Pb dates within LA-ICPMS uncertainty. Concordant analyses in both treated and un-treated aliquots have  
168 similar U concentrations suggesting that zones with high U concentrations (Tables S1-S13) were not selectively  
169 removed by chemical abrasion despite the correlation between high U concentrations, radiation damage, and Pb-loss  
170 (e.g., Widmann et al., 2019). However, reference materials are chosen for their homogeneous nature regarding isotopic  
171 compositions, so it is not surprising that U concentrations are indistinguishable between the two aliquots. The  
172 reproducibility of U-Pb dates for all of the reference materials is strong evidence that a single primary reference  
173 material (FC-1 in this case) can be used to correct for instrumental fractionation across a wide range of zircon ages, U  
174 content, and trace element compositions for chemically abraded zircon.



175



176

177

178 **Figure 1.** Comparison of  $^{206}\text{Pb}/^{238}\text{U}$  and  $^{207}\text{Pb}/^{206}\text{Pb}$  (CA)-LA-ICP-MS ages with CA-ID-TIMS ages for thirteen  
 179 reference materials that range in age from 28 to 3467 Ma. Each square is the weighted mean of a set of (CA)-LA-ICP-  
 180 MS measurements shown as the percent offset from the known reference age (ID-TIMS). The uncertainty is reported  
 181 as 2-sigma standard error of the weighted mean. Chemical abrasion of treated aliquots was conducted at Purdue  
 182 University and laser ablation analyses were conducted at Arizona LaserChron Center on the Thermo Element2 single-  
 183 collector ICP-MS. Methods for LA-ICP-MS at LaserChron using the Element2 are described by Pullen et al. (2018).



184

185           The scatter in the CA-LA-ICP-MS dates for both treated and untreated aliquots is similar for all age ranges.  
186   The greatest scatter in calculated weighted mean ages (~4 to 0.2% age offset from reference date) is in both the treated  
187   and untreated Mesozoic to Cenozoic reference materials. This scatter in age offset is improved by chemical abrasion  
188   for Paleozoic reference materials (2.0 to -0.8% age offset) and excellent for Proterozoic and Archean aliquots (0.6%  
189   to -0.7%). However, when comparing treated and untreated aliquots, the behavior of some reference materials warrants  
190   further discussion below. The CA-LA-ICP-MS weighted mean  $^{206}\text{Pb}/^{238}\text{U}$  dates for two Cenozoic reference materials  
191   were older than the CA-ID-TIMS reference date. Chemical abrasion of GHR1 zircon led to increased concordance,  
192   but an older  $^{206}\text{Pb}/^{238}\text{U}$  weighted mean date (Fig. A2). We attribute this difference to the presence of slightly older  
193   xenocrysts within the sample (e.g., Eddy et al., 2019). We see a similar result for Fish Canyon tuff zircon where the  
194   CA aliquot showed increased concordance, but the calculated mean age was offset more from the reference age than  
195   the no-CA aliquot (Fig. S1). This sample contains significant antecrysts that might bias its results (e.g., Wotzlaw et  
196   al., 2013). Indeed, increased precision and accuracy in analyses of young suites of igneous zircon routinely find  
197   overdispersion that can be related to protracted zircon growth or the presence of xenocrysts/antecrysts. Thus, the slight  
198   variability in weighted mean dates for GHR1 and Fish Canyon samples in CA-LA-ICP-MS analyses is not entirely  
199   unexpected and therefore unlikely to reflect of a systematic bias of the CA-LA-ICPMS method.

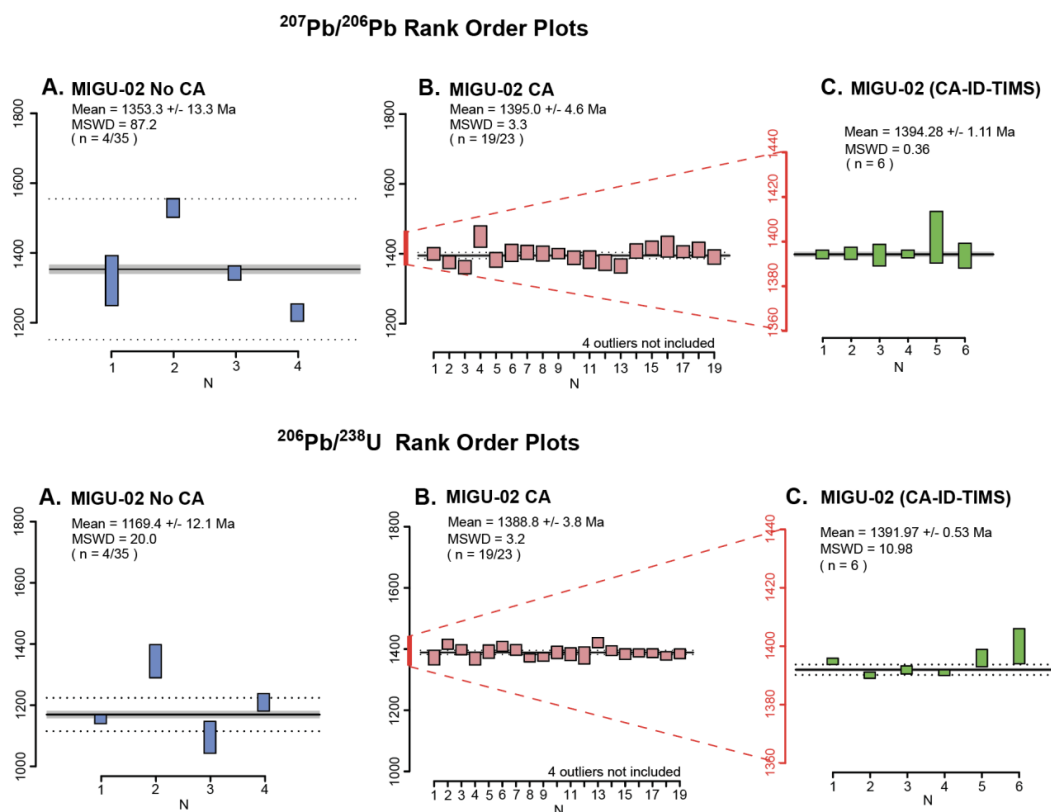
200

### 201 **3.2 Untreated and CA- U-Pb Zircon LA-ICP-MS Analyses of Metamict Zircon**

202           A Precambrian granite sample from the Parguaza Complex in the North Guyana Shield (MIGU-02; N 5° 21'  
203   3.70"; W 67° 41' 33.41") that has experienced substantial radiation damage was analyzed to assess the effects of  
204   chemical abrasion on grains with significant Pb-loss. Untreated (n = 35) and treated aliquots (n = 23) of MIGU-02  
205   were analyzed at the ALC and compared to a reference age determined by CA-ID-TIMS at Purdue University  
206   (n=6)(Fig. 2; Tables S14 and S15). During the bulk chemical abrasion process, 80-85% of MIGU-02 grains fully  
207   dissolved, leaving only a small fraction of the original aliquot to be used for analyses.

208





209

210 **Figure 2.** Rank order plots of calculated  $^{207}\text{Pb}/^{206}\text{Pb}$  and  $^{206}\text{Pb}/^{238}\text{U}$  ages for treated and untreated MIGU-02 aliquots  
211 and of the reference age for MIGU-02 obtained using CA-ID-TIMS. **A.** Untreated samples of MIGU-02 show large  
212 degree of scatter in dates and substantial deviation from the reference age. **B.** Treated zircons show a significant  
213 increase in precision and accuracy of ages relative to the reference age. **C.** Reference age for MIGU-02 determined  
214 using the weighted mean of six grains. See text for discordance criteria.

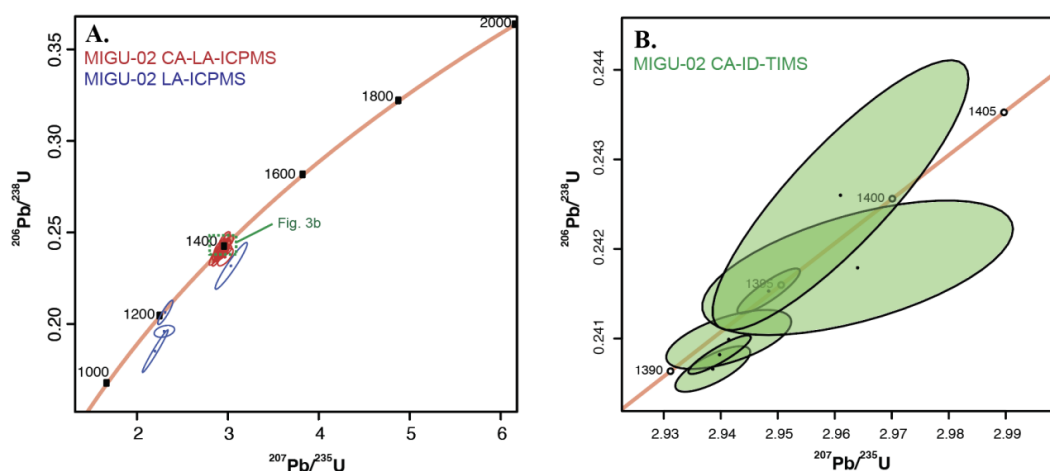
215

216 The  $^{207}\text{Pb}/^{206}\text{Pb}$  CA-ID-TIMS reference age for MIGU-02 is 1394.28 +/- 1.11 Ma (n=6, MSWD = 0.36),  
217 while the  $^{206}\text{Pb}/^{238}\text{U}$  dates are more scattered (Fig. 2). The scatter indicates that U/Pb elemental fractionation occurred  
218 during chemical abrasion in one analysis (slight reverse discordance) and residual Pb-loss remained in others (normal  
219 discordance)(Fig. 3). Nevertheless, a weighted mean date of the  $^{206}\text{Pb}/^{238}\text{U}$  CA-ID-TIMS dates is 1391.97 +/- 0.53 Ma  
220 (n = 6, MSWD = 10.98) and indicates that residual Pb-loss only affects the dates at the <0.5% level. Untreated LA-  
221 ICP-MS analyses of MIGU-02 show significant discordance (Fig. 3) and only 4 analyses (n=4/20; 80% discordant)  
222 were retained after filtering by AgeCalcML v.1.42. Chemical abrasion substantially increased the number of  
223 concordant analyses (n = 23/23). Fifteen analyses were removed from the untreated aliquot dataset and seven analyses  
224 were removed from the treated aliquot dataset because they hit epoxy, and are not included in the totals. Although all  
225 grains were concordant in the treated aliquot, four grains were not included in the weighted mean because they had a





226 significantly older  $^{207}\text{Pb}/^{206}\text{Pb}$  dates (1571-1900 Ma) than the CA-ID-TIMS reference date (Table S14) and are likely  
227 xenocrystic. The weighted mean  $^{207}\text{Pb}/^{206}\text{Pb}$  date from the untreated MIGU-02 aliquot is  $1353.3 \pm 13.3$  Ma ( $n = 4/35$ ;  
228  $\text{MSWD} = 87.5$ ) and the treated aliquot is  $1395.0 \pm 4.6$  Ma ( $n = 19/23$ ;  $\text{MSWD} = 3.3$ ). The mean  $^{206}\text{Pb}/^{238}\text{U}$  date of  
229 the untreated aliquot is  $1169.4 \pm 12.1$  Ma ( $\text{MSWD} = 20.0$ ) and the mean  $^{206}\text{Pb}/^{238}\text{U}$  date of the treated aliquot is  
230  $1388.8 \pm 3.8$  Ma ( $\text{MSWD} = 3.2$ ). Thus, the dates from treated zircon show a significant increase in concordance,  
231 precision, and accuracy relative to the reference date as determined by CA-ID-TIMS (Fig. 2).  
232



233  
234 **Figure 3. A.** Untreated and treated aliquots of MIGU-02 shown on a concordia plot. Non-CA MIGU-02 dates are  
235 reversely discordant whereas CA dates fall on concordia and overlap the reference age. **B.** All CA-ID-TIMS analyses  
236 of MIGU-02 shown on a concordia plot. One date shows reverse discordance whereas all other dates fall on concordia  
237 or have slight normal discordance.

238  
239

240 When both untreated and treated MIGU-02 dates are plotted against uranium concentration, all the CA-  
241 treated analyses have low uranium concentrations (<500 ppm), while untreated grains show significant variation in  
242 uranium concentration (Fig. 4). Most of the high uranium concentration analyses from untreated zircon are  $>\pm 20\%$   
243 reversely discordant. Since uranium concentration is correlated to radiation damage in old zircon, this result reinforces  
244 the observation that CA is an effective tool for removing damaged zones of the zircon (Nasdala et al., 2005; Widmann  
245 et al., 2019).

246  
247  
248

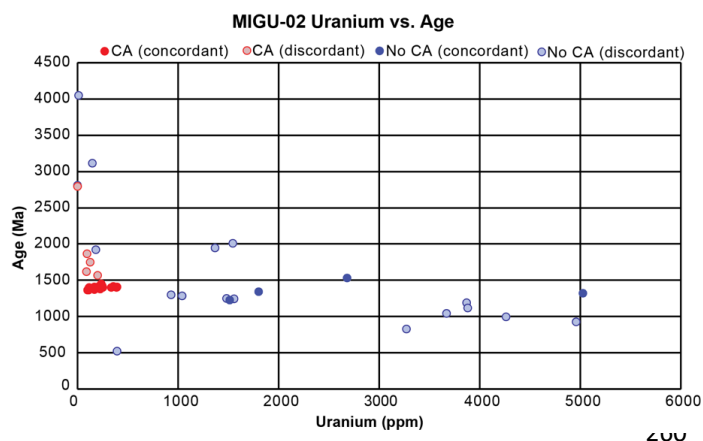


**Figure 4.** Uranium concentrations (ppm) plotted against  $^{207}\text{Pb}/^{206}\text{Pb}$  age (Ma) for both treated and untreated aliquots of MIGU-02. Both concordant and discordant analyses are shown. Uranium concentration is directly proportional with radiation damage in zircon with the same low-temperature cooling history. The restricted range of low U

261 concentrations in the CA-treated grains suggests that CA was effective at dissolving high U zircon that was more  
 262 likely to have Pb-loss.

263  
 264 **3.3 Untreated and CA- U-Pb Zircon LA-ICP-MS Analyses of Detrital Zircon**  
 265

266 One Phanerozoic (NM8A) and one Precambrian sample (Rora Med) were analyzed in this study to determine  
 267 how detrital zircon age distributions in samples with a wide range of age populations compare between chemically  
 268 abraded and untreated aliquots. We followed the ‘Large-n’ approach of Pullen et al. (2014) for this study, to obtain a  
 269 more robust distribution of ages, their modes, peak widths, and abundances of all analyzed samples – treated and  
 270 untreated. For NM8A, we analyzed 512 individual zircon in the treated aliquot and 896 zircon in the untreated aliquot.  
 271 In Rora Med, we analyzed 1035 zircon in the treated aliquot and 920 zircon in the untreated aliquot. Our results show  
 272 that chemical abrasion (CA) changed the number and distribution of apparent peak age populations in both DZ samples  
 273 compared to the non-CA age spectra (Figs. 5 and 6). Most notably, the Phanerozoic age peaks in sample NM8A  
 274 narrowed, became more defined, and, in some cases, shifted to slightly older dates.

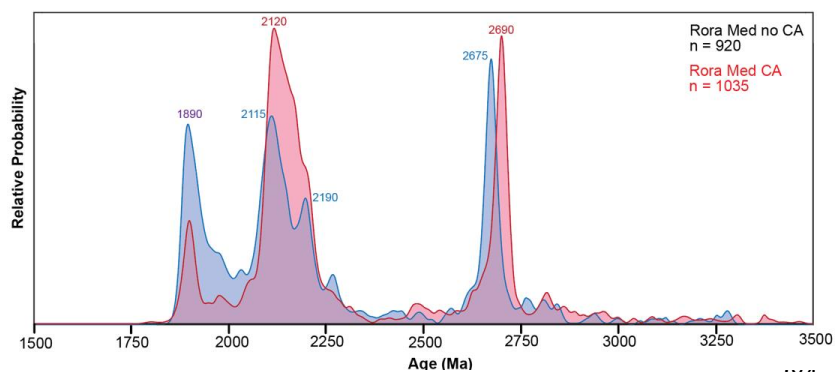


**Figure 5.** Comparison of U-Pb detrital zircon age spectra of not chemically abraded (blue) and chemically abraded (red) aliquots of Rora Med. Areas where age spectra overlap are shaded in purple. We aimed for

285 n=1000 for each aliquot because Pullen et al (2014) shows the distribution of analyzed zircon ages is thought to  
 286 approach the ‘true’ age distribution of the sample.



287 In the Precambrian sample (Rora Med), there are subtle changes in the DZ age spectra between the treated  
 288 and untreated aliquots. Overall, the CA treated aliquot shows improved concordance (Fig. 7) and age spectra show  
 289 narrowing of peak age populations, changes in the number of peaks present, and a slight but noticeable shift in peak  
 290 age populations to older ages (Fig. 5). Of note, the 1890 Ma peak narrows in the treated aliquot compared to the broad  
 291 peak that covers a range of ages between 1890 and 2000 Ma in the untreated aliquot. There is also a change in the  
 292 shape and number of peaks between the treated and untreated aliquots for the 2100-2300 Ma range. In the untreated  
 293 aliquot, there are three distinct peak age populations (~2115, 2190, & 2260 Ma), whereas in the treated aliquot, there  
 294 is only one broad peak age population that spans between ~2120-2190 Ma. There is also a distinct shift in the untreated  
 295 aliquot 2675 Ma peak age population to fifteen million years older in the treated aliquot (Fig. 5).  
 296

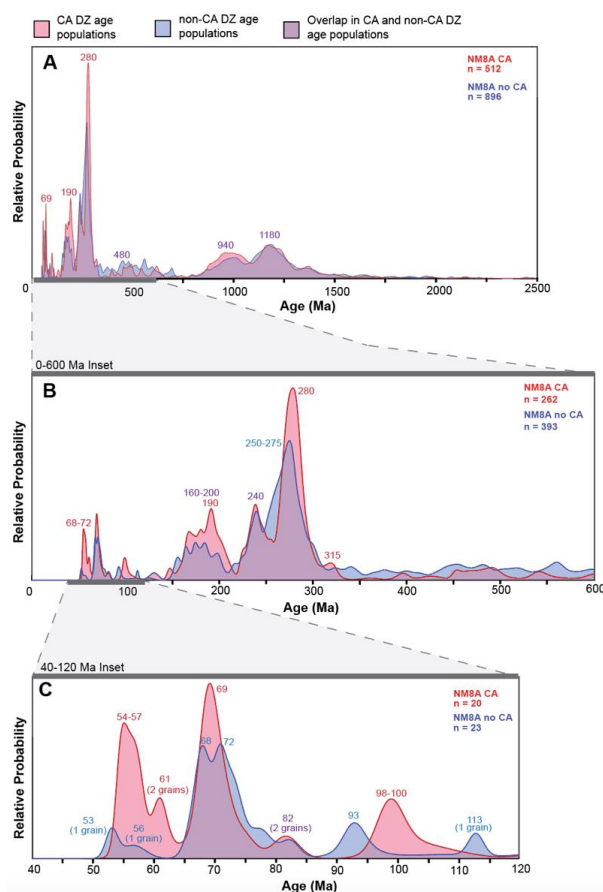


**Figure 6.** Comparison of U-Pb detrital age spectra of not chemically abraded (blue) and chemically abraded (red) aliquots of NM8A. Areas where age spectra overlap are shaded in purple. We aimed for n=1000 for each aliquot as the distribution of analyzed zircons ages is thought to approach the ‘true’ age distribution of the sample (Pullen et al. 2015). Insets A-C show variations of the scale on the x-axis.

There are also subtle changes in the number of peaks and peak shapes between the treated and untreated aliquots of NM8A. The most significant changes observed are increased resolution and definition of Phanerozoic peak age populations between 0 and 300 Ma for the treated aliquot (Fig. 6). For example, between 200-300 Ma, two broad peaks in the untreated aliquot sharpen and narrow to two well-defined peak age populations in the treated aliquot (Fig. 6b). Additionally, a broad population between 150

320 and 200 Ma in the untreated aliquot sharpens to a more distinct peak at 190 Ma, with two subordinate peaks between  
 321 150 and 175 Ma in the treated aliquot. We also see a zone of two broadly defined peaks at 68 and 72 Ma in the  
 322 untreated aliquot sharpen to a singular peak at 69 Ma in the treated aliquot. There is also an older shift from the 93  
 323 Ma peak in the untreated aliquot to ~98 Ma in the treated aliquot. Other shifts and changes in peak age populations



324 that are <120 Ma (Fig. 6c) cannot be confidently constrained due to the low number of analyses that define those  
325 populations (1-2 grains). Concordance is indistinguishable between treated and untreated aliquots of NM8A (Fig. 7).  
326  
327

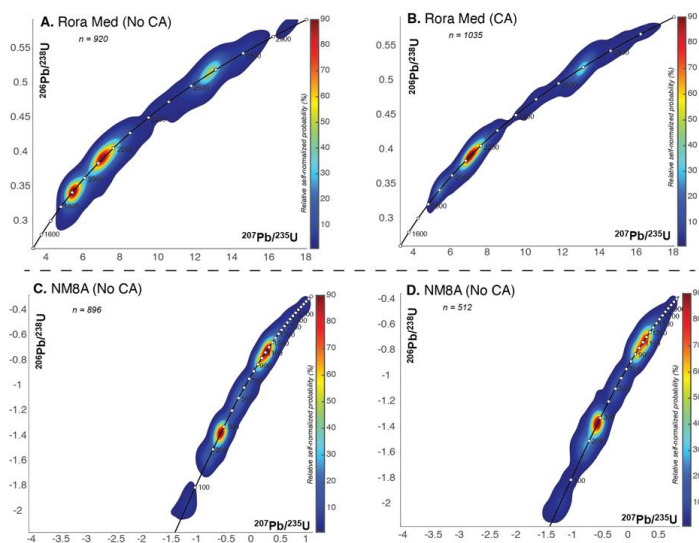


**Figure 7.** Density contour concordia diagrams for not chemically abraded and chemically abraded aliquots of detrital zircon samples NM8A and Rora Med (A-D). There is substantial improvement in concordance of the Proterozoic Rora Med sample from the not chemically abraded to the chemically abraded aliquot (A-B). However, both aliquots of the Phanerozoic NM8A sample are indistinguishable (C-D). Please note that the concordia diagrams for NM8A (C-D) are plotted on a

342 logarithmic scale.

343

344

345

346

#### 4. Discussion

347

348

349

350

351

352

353

354

355

356

357

358

359

360

Our study shows that chemical abrasion prior to LA-ICP-MS analysis does not negatively affect resulting U-Pb dates provided chemically abraded reference materials are used as the primary standard (e.g., Crowley et al., 2014; von Quadt et al., 2014). We also show that chemical abrasion is extremely effective in mitigating the effects of Pb-loss in LA-ICP-MS U-Pb dating of zircon that has experienced substantial radiation damage. Significant improvement was observed in both  $^{206}\text{Pb}/^{238}\text{U}$  and  $^{207}\text{Pb}/^{235}\text{U}$  dates of MIGU-02 zircon relative to ID-TIMS results, and also the efficiency of the analyses was dramatically improved by focusing LA-ICP-MS analyses on only those grains/fragments that survived the chemical abrasion process and had not sustained significant radiation damage. These results reinforce the observations of previous studies that used this approach (Crowley et al., 2014; von Quadt et al., 2014) and suggested that the CA-LA-ICP-MS method can be valuable for studies that need increased precision and accuracy in LA-ICP-MS U-Pb zircon analyses.

Given the apparent benefits of chemical abrasion to LA-ICP-MS analyses, it is natural to extend the technique to detrital zircon and test the advantages and disadvantages afforded by this method. Crowley et al. (2014) first used this approach on an Archean graywacke and showed that it did not significantly bias their results. However, this technique has not been widely used over the last decade. Our results indicate that a chemical abrasion pre-treatment may help resolve finer scale features in detrital zircon spectra from the Cenozoic to the Archean. We attribute this



361 increased resolution mainly to the mitigation of Pb-loss leading to increased accuracy of the resulting LA-ICP-MS  
362 dates.

363 We posit that mitigation of Pb-loss is behind the observed sharpening of Neoproterozoic through Cenozoic  
364 age populations in our samples because zircon dates in this age range are best determined using  $^{206}\text{Pb}/^{238}\text{U}$ , and the  
365 accuracy of this date can be compromised by Pb-loss that is difficult to identify since Pb-loss trajectories for zircon  
366 of this age range will closely follow concordia. These effects can be seen most clearly in sample NM8A where age  
367 peaks narrowed and became more defined (e.g., 250-300 Ma peak age populations) following chemical abrasion and  
368 some peak age populations shifted to slightly older dates (Fig. 6). Assuming that the zircons that form these  
369 populations cooled below the temperature at which radiation damage is effectively annealed at a similar time, then U  
370 content can be used as a proxy for radiation damage (Nasdala et al., 2005; Widmann et al., 2019; McKanna et al.,  
371 2023). This is clearly observed for the treated and untreated aliquots of igneous sample MIGU-02, where the treated  
372 aliquot has substantially lower U concentrations and increased accuracy and concordance of measured  $^{206}\text{Pb}/^{238}\text{U}$  dates  
373 (Figs. 2, 3, and 4). However, the thermal history is not known *a priori* for detrital zircon datasets, meaning this same  
374 assessment applied to NM8A and Rora Med is more uncertain.

375 To examine whether the reduced Pb-loss we observed in the chemically abraded aliquot reflects the selective  
376 dissolution of zircon with radiation damage, we compared zircon U concentrations from a particular age range (250-  
377 320 Ma) as a first-order approximation. We assume that the populations in this range likely have the same low-T  
378 cooling history, although with the caveat that this assumption remains unknown and cannot be tested with our data.  
379 We also note that these populations showed the most significant sharpening following chemical abrasion (Fig. 6B).  
380 Figure 8 shows that the average U concentration of treated grains in this age range is similar and indistinguishable to  
381 the untreated aliquot, indicating that we cannot determine if chemical abrasion selectively removed analyses that had  
382 Pb-loss. Note, however, that due to the unknown thermal history of the detrital zircon in this sample and sample NM8  
383 itself, it is much more difficult to directly compare U concentrations between detrital zircon aliquots than it is between  
384 igneous zircon from the same unit (e.g., MIGU-02) since we cannot assume that all zircons of the same age have  
385 experienced the same thermal history.

386

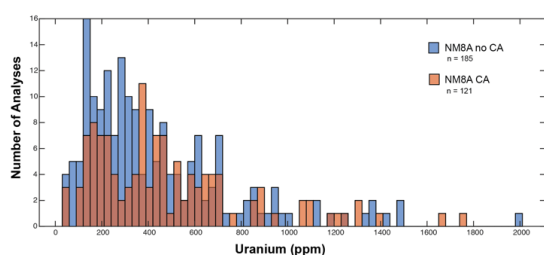


**Figure 8.** Histogram showing U concentration (ppm) for zircons in the peak age population between 250-320 Ma in detrital zircon sample NM8A. On the detrital zircon spectra, this age population narrows from one broad peak in the untreated aliquot to a well-defined, narrow peak in the treated aliquot (Fig. 6b). Measured U concentrations from this peak age population of

394 treated and untreated aliquots are overall similar and indistinguishable.

395

396 Reduced Pb-loss in Mesoproterozoic and older zircon also benefits detrital zircon studies because ancient  
397 Pb-loss can bias  $^{207}\text{Pb}/^{206}\text{Pb}$  dates of moderately discordant or even (analytically) concordant zircon toward



398 erroneously young values (Nemchin and Cawood, 2005). This effect has led many laboratories to filter for discordance  
399 within their datasets. Thus, improving concordance will increase the proportion of dates that can be retained in a  
400 detrital zircon study and improve confidence in the identification of peak age populations. One potential issue with  
401 this approach is the possibility that entire zircon populations will be removed during chemical abrasion if they have  
402 high degrees of radiation damage. Surprisingly, we did not see this effect in either NM8A nor Rora Med. This result  
403 is surprising and may be sample specific, since Rora Med zircon from all age populations have low U concentrations  
404 (<500 ppm; Fig. 9b). Although our RoraMed sample did not preferentially lose any age populations during CA, this  
405 feature may be unique to Precambrian samples with overall low zircon U concentrations and/or recent exhumation to  
406 low temperature conditions where radiation damage can accumulate and Pb-loss occurs.  
407

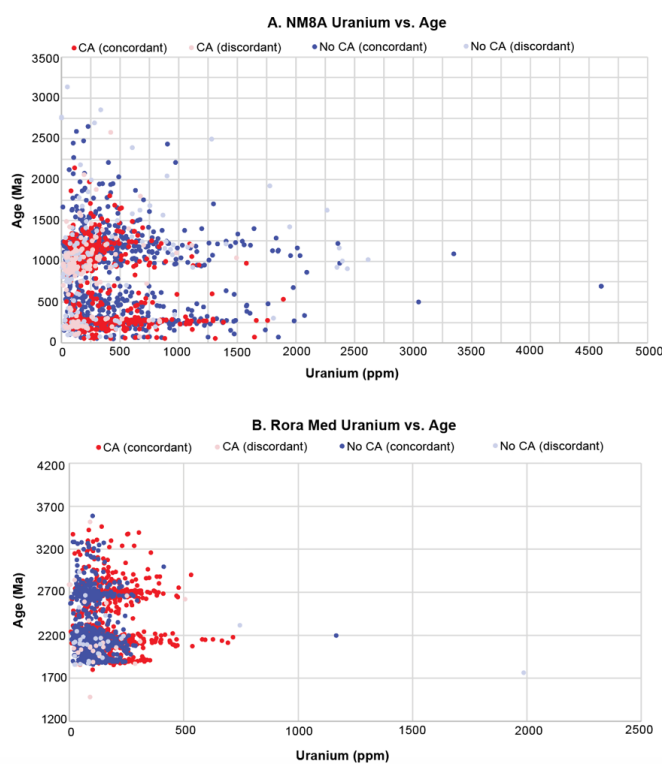


**Figure 9.** Scatter plot of uranium concentrations (ppm) plotted against the age (Ma) for both treated and untreated aliquots of **A.** NM8A and **B.** Rora Med. Both concordant and discordant analyses are shown. CA appears to reduce the scatter in U concentrations for Precambrian ages compared to the untreated aliquot in NM8A. Overall, all analyzed zircons in treated and untreated aliquots of Rora Med have low U concentrations (<500 ppm), and therefore minor differences in U concentrations are seen between treated and untreated aliquots.

42 /

428  
429 The nature of sediment transport may also work to remove metamict zircon prior to deposition in certain  
430 environments. Hydraulic sorting, mechanical abrasion, and weathering, can naturally bias detrital zircon populations  
431 present in a different lithologies (Malusa et al., 2013; Ibañez-Mejía et al., 2018). For example, Ewing et al. (2003)  
432 noted that metamictization leads to structural damage of the zircon crystal structure and that this can be correlated to  
433 a decrease in density and hardness. These changes lead metamict zircon to be more prone to destruction during river  
434 transport (Fedó et al., 2003; Hay and Dempster, 2009a). In particular, Hay and Dempster (2009a) argue that inclusion-



435 rich and metamict zircon are broken during sediment transport, and that these fragments do not survive being  
436 incorporated into clastic sandstone deposits. Instead, these smaller fragments can be swept out to more distal  
437 depositional environments. Small zircon are also typically lost during sample preparation (Hietpas et al., 2011; Slama  
438 and Kosler, 2012), meaning that both natural and laboratory processes may preferentially lead to a high proportion of  
439 undamaged zircon in sandstone samples. Thus, while we did not observe the removal of specific age populations  
440 following chemical abrasion in the two detrital zircon samples that were analyzed in this study and there are reasons  
441 to suspect that natural and laboratory processes will favor the analysis of undamaged zircon anyway, we recognize  
442 that other samples may behave differently. Future users of this technique should carefully consider this possibility in  
443 their datasets.

444 Another potential benefit of chemical abrasion is the preferential dissolution of inclusions within zircon  
445 during the partial dissolution step (McKanna et al., 2023). Inclusions harbor  $Pb_c$  that can be incorporated into the  
446 analyzed volume during laser ablation, reducing the  $Pb^*/Pb_c$  and limiting measurement precision and accuracy. When  
447 comparing the  $Pb^*/Pb_c$  ratios of treated and untreated aliquots of MIGU-02, we see a clear distinction that treated  
448 zircons have a much higher  $Pb^*/Pb_c$  ratio for similar ranges in U concentration (Fig. 10). We note that the overall U  
449 concentrations for the treated aliquot of MIGU-02 are low compared to the untreated aliquot, as we have already  
450 shown that CA for metamict zircon effectively removes high-U zones where Pb-loss is most likely to have occurred  
451 (see above discussion; Fig. 4). Regardless, the increased  $Pb^*/Pb_c$  ratio for the treated aliquot of MIGU-02 shows that  
452 this method is also efficient in removing inclusions with high  $Pb_c$  content and/or highly damaged domains where  $Pb_c$   
453 might have been introduced by fluids. These two effects are correlated with increased concordance, precision, and  
454 accuracy observed in  $^{206}Pb/^{238}U$  zircon dates of the treated aliquot of MIGU-02, supporting the benefits of utilizing  
455 CA prior to LA-ICP-MS measurements in metamict igneous zircon suites. It is likely that this same effect occurs in  
456 detrital zircons suites that are treated by chemical abrasion. Although, it is difficult to isolate since detrital zircons are  
457 sourced from various terranes and we cannot confidently compare the  $Pb^*/Pb_c$  of zircon with the same age, U  
458 concentration, and thermal history.

459

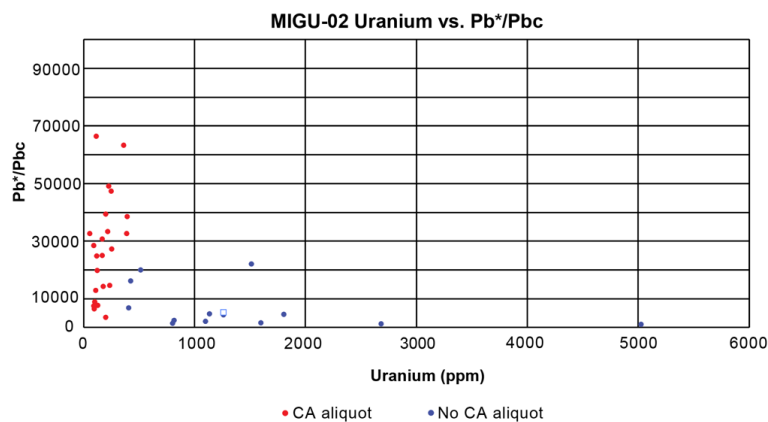


**Figure 10.**  $Pb^*/Pb_c$  ratios are plotted against uranium for MIGU-02. The  $Pb^*/Pb_c$  ratios in the treated aliquot of MIGU-02 are significantly higher than the untreated aliquot for similar concentrations of U. Higher  $Pb^*/Pb_c$  ratios in the treated aliquot of MIGU-02 can be attributed to reduction of  $Pb_c$  by

471 removal of inclusions.





## 472 **5. Conclusions and Recommended Applications**

473 Chemical abrasion is a widely used tool in the zircon U-Pb ID-TIMS community (*see reviews in* Schoene,  
474 2014; Schaltegger et al., 2015), where it has been repeatedly shown to mitigate the negative effects on age accuracy  
475 introduced by Pb-loss (Mundil et al., 2004; Mattinson, 2005; Widmann et al., 2019). Recent efforts to extend chemical  
476 abrasion to LA-ICP-MS analyses have also shown that this pre-treatment can be beneficial (Crowley et al., 2014; Von  
477 Quadt et al., 2014; McKanna et al., 2023; Sharman and Malkowski, 2023). The extension of this pre-treatment to  
478 large-n detrital zircon analyses is a natural outgrowth of these efforts. Our results indicate no negative effects from  
479 chemical abrasion prior to LA-ICP-MS analyses and that the technique results in improved concordance, precision,  
480 and, at least for the highly radiation damaged igneous sample we studied here, accuracy of measured U-Pb dates. For  
481 DZ samples, these benefits appear to translate to more defined and slightly older  $^{206}\text{Pb}/^{238}\text{U}$  age peaks for Phanerozoic  
482 zircon, and more concordant analyses, and in some cases slightly older  $^{207}\text{Pb}/^{206}\text{Pb}$  dates, for Precambrian zircon. One  
483 potential drawback of this pre-treatment is the possibility that age populations characterized by high-U zircon may be  
484 selectively dissolved during chemical abrasion. We did not observe this effect in either of our tested samples.  
485 However, we remain wary of its possibility in other samples with highly damaged Precambrian zircon populations,  
486 and so future practitioners are advised caution. The differences between age distributions in our analyzed detrital  
487 zircon spectra are slight and indicate that the Pb-loss present in typical untreated analyses would not significantly alter  
488 the interpretation of sediment source terranes at a broad scale. However, chemical abrasion did sharpen several  
489 Phanerozoic peak ages and increased concordance in Precambrian zircon populations, indicating that the pre-treatment  
490 may be useful in certain scenarios in which researchers may require increased resolution of detrital zircon age spectra  
491 to distinguish fine-scale variations in provenance, sediment source terranes, or source characteristics.

492

### 493 **Supplement**

494 All datasets utilized in this study are available in the Supplementary Material online at:

495

### 496 **Author contribution**

497 EED and MPE designed experiments and EED conducted the experiments. All authors participated in the  
498 interpretation and discussion of results. EED prepared the figures and manuscript.

499

### 500 **Competing Interests**

501 The authors declare no competing interests.

502

### 503 **Acknowledgments**

504 We thank the Arizona LaserChron Center (ALC) for sharing samples and reference materials and for helping  
505 analyze these samples. Specifically, we thank G. Gehrels, M. Pecha, D. Alberts, and Wai Allen. We also thank R.  
506 Ickert for help designing a system for bulk CA at Purdue. All LA-ICPMS measurements were made at the Arizona  
507 LaserChron Center under NSF-EAR 2050246 for support of the Arizona LaserChron Center and all CA steps and  
508 CA-ID-TIMS measurements were completed at Purdue University's Radiogenic Isotope Geology Lab (RIGL) under  
509 NSF-EAR-2151277 to M. Eddy.



510 **References**

- 511 Anderson, T.: Detrital zircons as tracers of sedimentary provenance: limiting conditions from statistics and  
512 numerical simulation, *Chemical Geology*, 216, 249–270, doi: <https://doi.org/10.1016/j.chemgeo.2004.11.013>, 2005.  
513
- 514 Balan, E., Neuville, D.R., Trocellier, P., Fritsch, E., Muller, J. P., Calas, G.: Metamictization and chemical durability  
515 of detrital zircon, *Am. Mineral.*, 86, 1025-1033, 2001.  
516
- 517 Black, L.P., Kamo, S.L., Allen, C.M., Aleinikoff, J.N., Davis, D.W., Korsch, R.J., and Foudoulis, C.: TEMORA-1:  
518 A new zircon standard for Phanerozoic U-Pb geochronology, *Chemical Geology*, 200, 155-170, 2003.  
519
- 520 Black, L.P., Kamo, S.L., Allen, C.M., Davis, D.W., Aleinikoff, J.N., Valley, J.W., Mundil, R., Campbell, I.H.,  
521 Korsch, R.J., Williams, I.S., and Foudoulis, C.: Improved <sup>206</sup>Pb/<sup>235</sup>U microprobe geochronology by the  
522 monitoring of a trace-element-related matrix effect; SHRIMP, ID-TIMS, ELA-ICP-MS and oxygen isotope  
523 documentation for a series of zircon standards, *Chemical Geology*, 205, 115-140, doi:  
524 <https://doi.org/10.1016/j.chemgeo.2004.01.003>, 2004  
525
- 526 Bowring, J.F., McLean, N.M., and Bowring, S.A.: Engineering cyber infrastructure for U-Pb geochronology: Tripoli  
527 and U-Pb redux, *Geochemistry, Geophysics, and Geosystems*, 12, doi: <https://doi.org/10.1029/2010GC003479>, 2011  
528
- 529 Carrapa, B., 2010: Resolving tectonic problems by dating detrital minerals, *Geology*, 38, 191–92, doi:  
530 <https://doi.org/10.1130/focus022010.1>, 2010  
531
- 532 Condon, D.J., Schoene, B., McLean, N.M., Bowring, S.A., and Parrish, R.R.: Metrology and traceability of U-Pb  
533 isotopic dilution geochronology (EARTHTIME tracer calibration part 1), *Geochimica et Cosmochimica Acta*, 164,  
534 464-480, 2015  
535
- 536 Crowley J.L., Schoene, B., and Bowring, S.A: U–Pb dating of zircon in the Bishop  
537 Tuff at the millennial scale, *Geology*, 35, 1123–1126, doi: <https://doi.org/10.1130/G24017A.1>, 2007  
538
- 539 Crowley, Q.G., Heron, K., Riggs, N., Kamber, B., Chew, D., McConnell, B., and Benn, K.: Chemical Abrasion  
540 Applied to LA-ICP-MS U-Pb Zircon Geochronology, *Minerals*, 4, 503-518, doi:  
541 <https://doi.org/10.3390/min4020503>, 2014  
542
- 543 Eddy, M.P., Ibañez-Mejía, M., Burgess, S.D., Coble, M.A., Cordani, U.G., DesOrmeau, J., Gehrels, G.E., Li, X.,  
544 MacLennan, S., Pecha, M., Sato, K., Schoene, B., Valencia, V.A., Vervoort, J.D., and Wang, T.: GHR1 Zircon – A  
545 New Eocene Natural Reference Material for Microbeam U-Pb Geochronology and Hf Isotopic Analysis of Zircon,  
546 *Geostandards and Geoanalytical Research*, 43, 113-132, doi: <https://doi.org/10.1111/ggr.12246>, 2019.  
547
- 548 Ewing, R.C., Meldrum, A., Wang, L., Weber, W.J., Corrales, I.R.: Radiation effects in zircon In Hanchar, J.M.,  
549 Hoskin, P.W.O. (Eds.), *Zircon. Rev. Mineral. Geochem.*, 53, *Mineral Society of America*, 277-303, 2003.  
550
- 551 Fedo C.M., Sircombe, K., and Rainbird, R.: Detrital zircon analysis of the sedimentary record, *Reviews in*  
552 *Mineralogy and Geochemistry*, 53, 277-303, doi: <https://doi.org/10.2113/0530277>, 2003  
553
- 554 Gehrels, G.E.: Detrital zircon U-Pb geochronology: current methods and new opportunities, In *Tectonics of*  
555 *Sedimentary Basins: Recent Advances*, eds C., Busby, A., Azor, pp. 47–62, Chichester, UK: Wiley-Blackwell, 2012  
556
- 557 Gehrels, G.E., Valencia, V., Ruiz, J.: Enhanced precision, accuracy, efficiency, and spatial resolution of U-Pb ages  
558 by laser ablation–multicollector–inductively coupled plasma–mass spectrometry, *Geochemistry, Geophysics, and*  
559 *Geosystems*, 9, doi: <https://doi.org/10.1029/2007GC001805>, 2008  
560
- 561 Gehrels, G.E.: Detrital zircon U-Pb Geochronology Applied to Tectonics: *Annual Review of Earth and Planetary*  
562 *Sciences*, 42, 127-149, doi: <https://doi.org/10.1146/annurev-earth-050212-124012>, 2014  
563



- 564 Gehrels, G.E., and Pecha, M.: Detrital zircon U-Pb geochronology and Hf isotope geochemistry of Paleozoic and  
565 Triassic passive margin strata of western North America, *Geosphere*, 10, 49–65, doi:  
566 <https://doi.org/10.1130/GES00889.1>, 2014  
567  
568 Gehrels, G.E., Valencia, V., Pullen, A.: Detrital zircon U-Pb geochronology by Laser-Ablation Multicollector  
569 ICPMS at the Arizona LaserChron Center, in Loszewski, T., and Huff., W., eds., *Geochronology: Emerging*  
570 *Opportunities*, Paleontology Society Short Course: Paleontology Society Papers, 11, 2006.  
571  
572 Hay, D.C., and Dempster, T.J.: Zircon alteration, formation, and preservation in sandstones, *Sedimentology*, 56,  
573 2175-2191, doi: 10.1111/j.1365-3091.2009.01075.x, 2009.  
574  
575 Hay, D.C., and Dempster, T.J.: Zircon behaviour during low temperature metamorphism, *Journal of Petrology*, 50,  
576 571-598, 2009.  
577  
578 Hiess, J., Condon, D. J., McLean, N. and Noble, S. R.:  $^{238}\text{U}/^{235}\text{U}$  Systematics in Terrestrial Uranium-Bearing  
579 Minerals, *Science*, 335, 1610–1614, 2012  
580  
581 Hietpas, J., Samson, S., Moecher, D., Chakraborty, S.: Enhancing tectonic and provenance information from detrital  
582 zircon studies: assessing terrane-scale sampling and grain-scale characterization, *J. Geol. Soc. Lond.*, 168, 309-318,  
583 2011.  
584  
585 Ibañez-Mejía, M., Pullen, A., Pepper, M., Urbani, F., Ghoshal, G., and Ibañez-Mejía, J.C.: Use and abuse of detrital  
586 zircon U-Pb geochronology – A case from the Rio Orinoco delta, eastern Venezuela, *Geology*, 46, 1019-1022, 2018.  
587  
588 Jaffey, A.H., Flynn, K.F., Glendenin, L.E., Bentley, W.C., and Essling, A.M.: Precision Measurement of Half-Life  
589 and Specific Activities of  $^{235}\text{U}$  and  $^{238}\text{U}$ , *Physical Review C*, 4, 1971.  
590  
591 Malusa, M.G., Carter, A., Limoncelli, M., Villa, I. M., and Garzanti, E.: Bias in detrital zircon geochronology and  
592 thermochronometry, *Chemical Geology*, 359, 90-107, 2013.  
593  
594 Mattinson J.M.: Zircon U–Pb chemical-abrasion ("CA-TIMS") method: Combined annealing and multi-step  
595 dissolution analysis for improved precision and accuracy of zircon ages, *Chemical Geology*, 220, 47–56, doi:  
596 <https://doi.org/10.1016/j.chemgeo.2005.03.011>, 2005  
597  
598 Mattinson, J.M.: Analysis of the relative decay constants of  $^{235}\text{U}$  and  $^{238}\text{U}$  by multi-step CA-TIMS measurements  
599 of closed system natural zircon samples, *Chemical Geology*, 275, 186-198, doi:  
600 <https://doi.org/10.1016/j.chemgeo.2010.05.007>, 2010  
601  
602 McConnell, B., Riggs, N., and Crowley, Q.G.: Detrital zircon provenance and Ordovician terrane amalgamation,  
603 western Ireland, *Journal of the Geological Society*, 166, 473–484, doi: <https://doi.org/10.1144/0016-76492008-081>,  
604 2009  
605  
606 McKanna, A.J., Koran, I., Schoene, B., and Ketcham, R.A.: Chemical abrasion: the mechanics of zircon dissolution,  
607 *Geochronology*, 5, 127-151, <https://doi.org/10.5194/gchron-5-127-2023>, 2023  
608  
609 McLean, N.M., Condon, D.J., Schoene, B., and Bowring, S.A.: Evaluating uncertainties in the calibration of isotopic  
610 reference materials and multi-element isotopic tracers (EARTHTIME tracer calibration II), *Geochimica et*  
611 *Cosmochimica Acta*, 164, 481-501., 2015  
612  
613 Mundil, R., Ludwig, K.R., Metcalfe, I., and Renne, P.R.: Age and timing of the Permian mass extinctions: U/Pb  
614 dating of closed-system zircons, *Science*, doi: 10.1126/science.1101012., 2004  
615  
616 Nasdala, L., Hanchar, J.M., Kronz, A., Whitehouse, M.J.: Long-term stability of alpha particle damage in natural  
617 zircon, *Chemical Geology*, 220, 83-103, doi: <https://doi.org/10.1016/j.chemgeo.2005.03.012>, 2005  
618



- 619 Nemchin, A., and Cawood, P.: Discordance of the U-Pb system in detrital zircons: Implication for provenance  
620 studies of sedimentary rocks, *Sediment Geol.*, **182**, 143–162, 2005  
621
- 622 Parrish, R.R., and Noble, S.R.: Zircon U–Th–Pb geochronology by isotope dilution –Thermal ionization mass  
623 spectrometry (ID-TIMS): In Hanchar JM and Hoskin PWO (eds.) Zircon, *Reviews in Mineralogy and Geochemistry*,  
624 53, 183–213, Washington, DC: Mineralogical Society of America, 2003  
625
- 626 Pullen., A., Ibañez-Mejia, M., Gehrels, G.E., Ibanez-Mejia, J.C., and Pecha, M.: What happens when n=1000?  
627 Creating large-n geochronological datasets with LA-ICP-MS for geologic investigations, *Journal of Analytical*  
628 *Spectrometry*, 6, doi: <https://doi.org/10.1039/C4JA00024B>., 2014  
629
- 630 Pullen, A., Ibañez-Mejia, M., Gehrels, G.E., Giesler, D., and Pecha, M.: Optimization of a Laser Ablation-Single  
631 Collector-Inductively Coupled Plasma-Mass Spectrometer (Thermo Element 2) for Accurate, Precise, and Efficient  
632 Zircon U-Th-Pb Geochronology, *Geochemistry, Geophysics, and Geosystems*, 19, 3689-3705, 2018.  
633
- 634 Rahn, M.K., Brandon, M.T., Batt, G.E., Garver, J.I.: A zero damage model for fission-track annealing in zircon, *Am.*  
635 *Mineral.*, 89, 473-484, 2004.  
636
- 637 Schaltegger, U., Schmitt, A.K., and Horstwood, M.S.A.: U-Th-Pb zircon geochronology by ID-TIMS, SIMS, and  
638 laser ablation ICP-MS: recipes, interpretations, and opportunities, *Chem. Geol.*, 402, 89-110,  
639 <https://doi.org/10.1016/j.chemgeo.2015.02.028>, 2015  
640
- 641 Schmitz, M.D., and Bowring, S.A.: U-Pb zircon and titanite systematics of the Fish Canyon Tuff: an assessment of  
642 high-precision U-Pb geochronology and its application to young volcanic rocks, *Geochimica et Cosmochimica Acta*,  
643 65, 2571-2587, 2001  
644
- 645 Schoene, B.: U-Th-Pb Geochronology, Treatise on geochemistry 2<sup>nd</sup> edition, doi: [http://dx.doi.org/10.1016/B978-0-](http://dx.doi.org/10.1016/B978-0-08-095975-7.00310-7)  
646 [08-095975-7.00310-7](http://dx.doi.org/10.1016/B978-0-08-095975-7.00310-7), 2014  
647
- 648 Smith, T.M., Saylor, J.E., Lapen, T.J., Leary, R.J., and Sundell, K.E.: Large detrital zircon data set investigation and  
649 provenance mapping: Local versus regional and continental sediment sources before, during, and after Ancestral  
650 Rocky Mountain deformation, *GSA Bulletin*, doi: <https://doi.org/10.1130/B36285.1>, 2023  
651
- 652 Sláma, J., Kosler, J., Condon, D.J., Crowley, J.L., Gerdes, A., Hanchar, J.M., Horstwood, M.S.A., Morris, G.A.,  
653 Nasdala, L., Norberg, N., Schaltegger, U., Schoene, B., Tubrett, M.N., and Whitehouse, M.J.: Plesovice zircon – A  
654 new natural reference material for U-Pb and Hf isotopic microanalysis, *Chemical Geology*, 249, 1-35, doi:  
655 <https://doi.org/10.1016/j.chemgeo.2007.11.005>, 2008  
656
- 657 Slama, J., and Kosler, J.: Effects of sampling and mineral separation on accuracy of detrital zircon studies,  
658 *Geochemistry, Geophysics, Geosystems*, 13, 2012.  
659
- 660 Stern, R.A., Bodorkos, S., Kama, S.L., Hickman, A.H., and Corfu, F.: Measurement of SIMS instrumental mass  
661 fractionation of Pb isotopes during zircon dating, *Geostandards and Geoanalytical Research*, 33, 145-168, doi:  
662 <https://doi.org/10.1111/j.1751-908X.2009.00023.x>, 2009  
663
- 664 Sundell, K. E., Gehrels, G. E., and Pecha, M. E.: Rapid U-Pb Geochronology by Laser Ablation Multi-Collector  
665 ICP-MS, *Geostand Geoanal Res.*, 45, 37–57, 2021  
666
- 667 Von Quadt, A., Dallhofer, D., Guilong, M., Peytcheva, I., Waelle, M., and Sakata, S.: U-Pb dating of CA/non-CA  
668 treated zircons obtained by LA-ICP-MS and CA-TIMS techniques: impact for their geological interpretation,  
669 *Journal of Analytical Atomic Spectrometry*, 29, 1618-1629, doi: <https://doi.org/10.1039/C4JA00102H>, 2014  
670
- 671 Wang, J. W., Gehrels, G., Kapp, P. & Sundell, K.: Evidence for regionally continuous Early Cretaceous sinistral  
672 shear zones along the western flank of the Coast Mountains, coastal British Columbia, Canada, *Geosphere*, 19, 139–  
673 162, 2022.  
674



- 675 Wiedenbeck, M., Alle, P., Corfu, F., Griffin, W.L., Meier, M., Oberli, F., von Quadt, A., Roddick, J.C., and Spiegel,  
676 W.: Three natural zircon standards for U-Th-Pb, Lu-Hf, trace element and REE analyses, *Geostandards Newsletter*,  
677 v. 19, p. 1-23, 1995  
678  
679 Widmann, P., Davies, J.H.F.L., and Schaltegger, U.: Calibrating chemical abrasion: Its effects on zircon crystal  
680 structure, chemical composition and U-Pb age, *Chemical Geology*, 511, 1-10,  
681 <https://doi.org/10.1016/j.chemgeo.2019.02.026>, 2019  
682  
683 Wiedenbeck, M., Hanchar, J.M., Peck, W.H., Sylvester, P., Valley, J., Whitehouse, M., Kronz, A., Morishita, Y.,  
684 Nasdala, L., Fiebig, J., Franchi, I., Girard, J.P., Greenwood, R.C., Hinton, R., Kita, N., Mason, P.R.D., Norman, M.,  
685 Ogasawara, M., Piccoli, P.M., Rhede, D., Satoh, H., Schultz-Dobrick, B., Skar, O., Spicuzza, M.J., Terada, K.,  
686 Tindle, A., Togashi, S., Vennemann, T., Xie, Q., and Zheng, Y.F.: Further characterization of the 91500 zircon  
687 crystal, *Geostandards and Geoanalytical Research*, v. 28, p. 9-39, doi: [https://doi.org/10.1111/j.1751-](https://doi.org/10.1111/j.1751-908X.2004.tb01041.x)  
688 [908X.2004.tb01041.x](https://doi.org/10.1111/j.1751-908X.2004.tb01041.x), 2004  
689  
690 Wotzlaw, J.F., Schaltegger, U., Frick, D.A., Dungan, M.A., Gerdes, A., and Gunther, D.: Tracking the evolution of  
691 large-volume silicic magma reservoirs from assembly to supereruption, *Geology*, 41, 867-870, 2013  
692